Tunable Kondo Physics in a Carbon Nanotube Double Quantum Dot

S. J. Chorley,[1] M. R. Galpin,[2] F. W. Jayatilaka,[2] C. G. Smith,[1] D. E. Logan,[2] and M. R. Buitelaar[1]

[1]*Cavendish Laboratory, University of Cambridge, Cambridge CB3 0HE, United Kingdom*
[2]*Department of Chemistry, Physical and Theoretical Chemistry Laboratory, University of Oxford, Oxford OX1 3QZ, United Kingdom*

We investigate a tunable two-impurity Kondo system in a strongly correlated carbon nanotube double quantum dot, accessing the full range of charge regimes. In the regime where both dots contain an unpaired electron, the system approaches the two-impurity Kondo model. At zero magnetic field the interdot coupling disrupts the Kondo physics and a local singlet state arises, but we are able to tune the crossover to a Kondo screened phase by application of a magnetic field. All results show good agreement with a numerical renormalization group study of the device.

PACS numbers: 73.63.Kv, 72.15.Qm, 73.23.Hk, 73.63.Fg

A quantum dot coupled to two leads can be considered as an experimental realization of the single-impurity Anderson model [1]. When the dot contains a single unpaired electron, the Anderson model accurately describes how, below a characteristic temperature T_K, correlated electron tunnelling between the quantum dot and the leads results in coherent screening of the electron spin [2–4]. The combined system of electrons on the quantum dot and leads forms a spin singlet, a phenomenon known as the Kondo effect [5]. Likewise, two tunnel-coupled quantum dots should amount to an experimental realization of the two-impurity Anderson model [6]. Here the physics is much richer, particularly in the regime where each dot contains an unpaired electron. In this case, a competition now arises between the tendency of the conduction electrons on the leads to screen the spins on the quantum dots, and the antiferromagnetic exchange coupling J between the two localized spins. The former favors formation of a Kondo singlet between each lead and the dot to which it is coupled, while the latter favors a local singlet state. The resulting ground state of the system depends sensitively on the relative strength of the interactions, an understanding of which is important and believed to underlie the electronic properties of a wide range of strongly correlated materials, including spin glasses and heavy fermion compounds [5].

The essence of this competition is captured by the two-impurity Kondo model [7–10], which describes the low-energy physics of the two-impurity Anderson model in the absence of charge transfer between the leads, and famously contains a quantum phase transition at the boundary of the local and Kondo singlet phases where $J \sim T_K$. While this has attracted considerable experimental attention [11–13], observation of the transition has remained elusive. This is perhaps unsurprising as charge transfer between the leads, absent in the two-impurity Kondo model, is necessarily present in experiment if a conductance is measured. As is well known theoretically, this transforms the quantum phase transition into a crossover, such that the ground state

of the system is always a Fermi liquid [10,14], although remnants of the transition are evident in a strong enhancement of the zero-bias conductance in the vicinity of $J \sim T_K$ [15–17].

An understanding of the transport properties of a realistic two-impurity system, such as a double quantum dot (DQD), thus requires that charge transfer between the leads be taken into account. This is achieved in the present Letter, where we present a study of a tunable carbon nanotube DQD in the strongly correlated regime, and use a numerical renormalization group (NRG) study of the two-impurity Anderson model to describe the device. We show that in the charge regime where both dots have an unpaired electron, the ground state of the device is a local singlet phase with suppressed Kondo correlations. The ability to tune the exchange coupling and the Kondo scales allows one, in principle, to cross over from the local singlet to the Kondo screened phase. In our device the onset of charge fluctuations prevents the crossover being seen cleanly at zero magnetic field. We have, however, been able to observe it at finite magnetic field, consistent with recent theoretical predictions [14].

The device we consider is a single-walled carbon nanotube on a degenerately doped Si/SiO$_2$ substrate contacted by Au contacts, see Fig. 1(a) [18]. A central gate is used to introduce a tunable tunnel barrier, separating the nanotube into two quantum dots, which can be individually addressed by two additional side gates. The stability diagram of the device is shown in Fig. 1(b). The effective electron number of each charge regime is indicated by the ordered pairs (n, m). The large-small-large alternation in the stability diagram reflects the twofold spin degeneracy of the device, and allows us to establish unambiguously the parity of the electron number (even or odd). The orbital degeneracy of the nanotubes is broken, most likely as a result of $K - K'$ mixing [19,20].

From an analysis of the stability diagram we are able to extract the on-site charging energies $U \sim 2.5$ meV for both dots, the electrostatic coupling energy $U' \sim 0.6$ meV, and
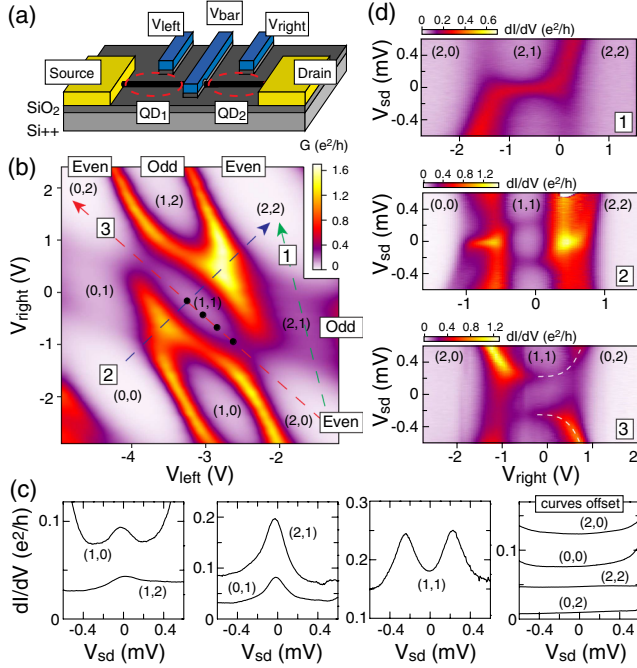
FIG. 1 (color online). (a) Schematic of the carbon nanotube DQD device. (b) Stability diagram of the DQD measured at $T \sim 60$ mK. The Si backgate voltage $V_{bg} = -1.7$ V. The barrier gate voltage $V_{bar} = 0$ mV. (c) Differential conductance in the centers of the various charge regimes of panel (b) as indicated by (n, m). The curves in the rightmost panel are offset in steps of 0.03 e^2/h. (d) Differential conductance along the lines indicated in panel (a).

the interdot tunnel coupling $t \sim 0.4$ meV. The widths of the Coulomb blockade peaks in the stability diagram allow an estimate of the coupling Γ between the dots and the leads. In the noninteracting limit the full width at half maximum is equal to 2Γ, but the peaks are broadened by a further factor of ~ 2 by many-body scattering processes [21]. Bearing this in mind, we obtain $\Gamma_R \sim 0.23$ meV and $\Gamma_L \sim 0.12$ meV for the right and left dot, respectively. For these coupling strengths $U/\Gamma_\nu \sim 10$, so we might expect cotunneling processes, and thus the Kondo effect, to be experimentally observable. To investigate the presence of Kondo correlations, we measured the differential conductance in all charge regimes, see Figs. 1(c) and 1(d). When both dots contain an even number of electrons, the Kondo effect is inoperative, and conductance is suppressed and featureless around the source-drain bias $V_{sd} = 0$. On the other hand, when *one* of the quantum dots contains an odd number of electrons, we observe a pronounced zero-bias conductance peak. The evolution of the differential conductance as electrons are added to the right dot, keeping the effective electron number of the left dot fixed at $N = 2$, is shown in the topmost panel of Fig. 1(d). The characteristic appearance of a zero-bias peak when the electron number is odd is a clear indication of Kondo physics in the (0,1), (1,0), (1,2), and (2,1) charge regimes [2–4], the

spin of the singly occupied dot being effectively Kondo screened by the lead to which it is coupled.

The behavior, however, is markedly different in the center of the (1,1) charge regime where the electron number is odd for *both* dots. As shown in Fig. 1(c), the zero-bias conductance is suppressed and a double peak structure arises at finite bias [11,12]. The behavior we observe is characteristic of a strongly correlated DQD, when $J \gg T_K^L$, T_K^R, where T_K^L, T_K^R denote the Kondo scales for the left and right dots, respectively. These energy scales are readily estimated using the parameters obtained above. In the center of the (1,1) charge regime the exchange coupling $J \sim 4t^2/(U - U')$, which yields $J \sim 0.34$ meV. The Kondo scales can be estimated roughly using the Haldane expression [22]

$$T_K^\nu \sim \sqrt{\Gamma_\nu U} \exp[\pi \epsilon_\nu (\epsilon_\nu + U)/2\Gamma_\nu U], \tag{1}$$

where ϵ_ν ($\nu = L, R$) is the level energy of dot ν relative to the zero-bias Fermi level of the leads. This yields $T_K^R \sim 10^{-2}$ meV and $T_K^L \sim 10^{-4}$ meV in the middle of the (1,1) charge regime, such that $J \gg T_K^L, T_K^R$.

The above interpretation of the measurements is strengthened by an NRG study of our double quantum dot. The calculated stability diagram using the experimental parameters, see Fig. 2(a), reproduces all key features of the experiment and allows for a comparison between experiment and theory (for further details see the Supplemental Material [18]). Finite-bias conductances, the NRG calculation of which is inevitably approximate (see Ref. [18]), are also in good agreement. In particular the double peak structure in the (1,1) charge regime is reproduced in the calculations, see Fig. 2(b). It can be understood physically as a nonequilibrium Kondo
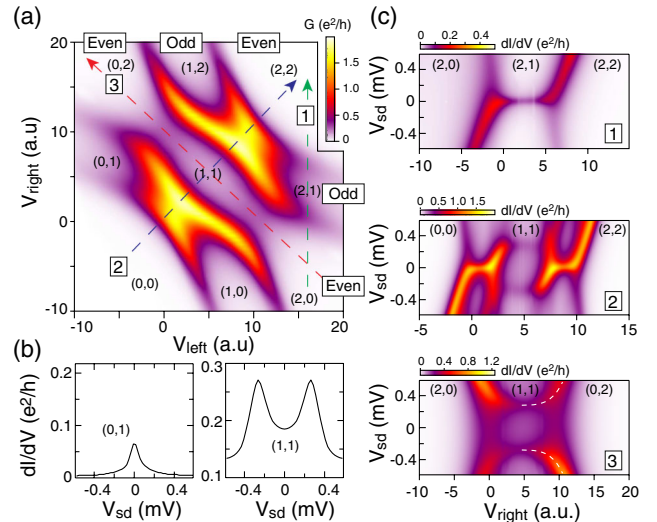

FIG. 2 (color online). (a) NRG calculation of the stability diagram. (b) Differential conductance in the centers of the various charge regimes of panel (a) as indicated by (n, m). (c) Differential conductance along the lines indicated in panel (a).

effect [23]. While the formation of a local singlet state suppresses Kondo correlations at zero bias, interlead spin-flip tunneling becomes possible and Kondo correlations are partially restored when V_{sd} is comparable to the exchange energy J separating the atomic-limit singlet ground state from its triplet excited states. As demonstrated below, a unique feature of double quantum dots is that T_K^L, T_K^R and J are all tunable by varying the dot level energies.

We discuss first the behavior along diagonal 2 in Fig. 1(b), for which the differential conductance is shown in Fig. 1(d), middle panel. Along this diagonal, the dot level energies $\epsilon_{L,R}$ are decreased while their difference (or detuning) $\epsilon_L - \epsilon_R$ remains zero. This allows us to tune the Kondo scales of the two quantum dots, as these strongly depend on the dot level energies, see Eq. (1). In the center of the (1,1) charge regime, the Kondo scales for both dots are at a minimum. Moving away from the center, the Kondo scales thus increase. However, before we can access the Kondo screened phase we reach the edge of the (1,1) charge regime, moving into a mixed-valence regime. Here charge fluctuations are significant, and a two-impurity Kondo model description is no longer valid. The inability to access the Kondo screened phase this way can be understood given that for our device $J \sim \Gamma_{L,R}$, so to observe the crossover requires $T_K^{L,R} \sim \Gamma_{L,R}$, which occurs only when $|\epsilon_{L,R}| \lesssim \Gamma_{L,R}$, i.e., in the mixed-valence regime. A lower J is therefore required in order to observe the crossover cleanly in this way. While we were able to control the tunnel coupling t experimentally (see Ref. [18]), sufficiently small values of it were not reached here.

We now focus on the behavior along diagonal 3 in Fig. 1(b) for which the differential conductance is shown in Fig. 1(d), bottom panel. Along this diagonal the detuning ($\epsilon_L - \epsilon_R$) is increased while $\epsilon_L + \epsilon_R$ is constant. As indicated by the dashed white line in Fig. 1(d), the peaks observed in the differential conductance move further apart as the magnitude of the detuning is increased and the conductance becomes highly asymmetric in bias. This increase in peak splitting is due to J becoming larger with positive detuning as the (1,1) singlet state becomes closer in energy to the (0,2) singlet [24]. The ability to tune the exchange energy by varying the detuning is essential in spin-based quantum information processing schemes using quantum dots [25]. Importantly, the present data show that this tunability can also be used as a probe of Kondo physics.

The consequences of varying the exchange J are investigated further in Fig. 3 by application of a magnetic field (B) perpendicular to the nanotube axis, for various values of the detuning along diagonal 3 in the (1, 1) regime. At finite B the observed zero-field peaks split into three components, Figure 3(a) [of which the innermost peaks are most easily resolved, see Figs. 3(a) and 3(b)], consistent with a local singlet ground state and triplet excited state, separated by $\sim J$ at $B = 0$. As B is increased, the energy
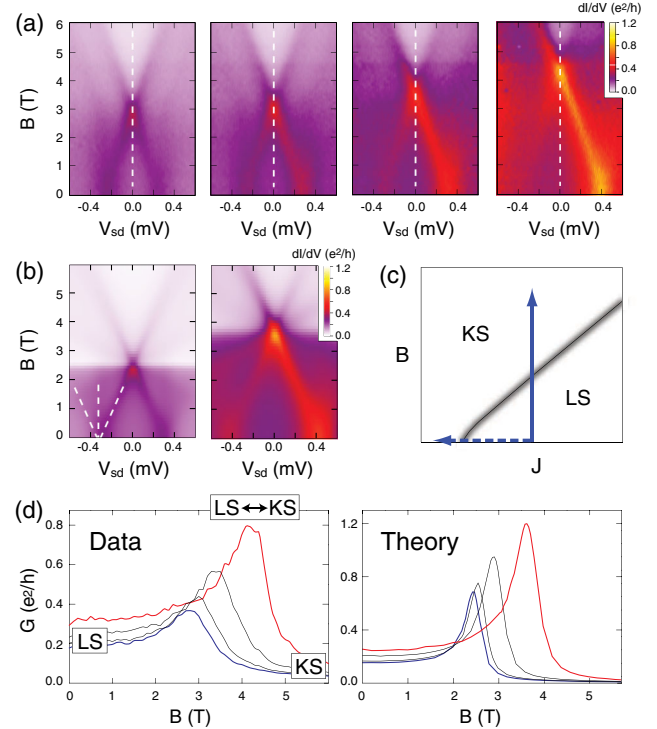

FIG. 3 (color online). (a) Magnetic field dependence of the differential conductance in the (1,1) charge regime for various values of the detuning as indicated by the black dots along line 3 in Fig. 1(b), with the left plot for the center of the (1,1) regime. (b) NRG results corresponding to the left and right panels in (a). Dashed lines show the threefold splitting of one zero-field peak. (c) Schematic of crossover between LS and KS phases, see text, either by varying B (solid arrowed line) or J (dashed arrowed line). (d) Zero-bias conductance vs B for different detuning, along dashed white lines in panel (a); both measured (left) and calculated (right). Individual curves from left to right correspond to (a) from left to right.

difference ($\sim J - g\mu_B B$) between the singlet (S) and the lowest-energy triplet state, T_-, decreases. At a field $B_c \sim J/g\mu_B$ these states are near degenerate. A strong zero-bias conductance peak is then observed, due to Kondo screening of the S-T_- pseudospin system [26–28], here by two channels. {In our tunnel-coupled double quantum dot both the S and T_- states arise from the (1, 1) charge configuration, in contrast to S-T_- crossings observed [4,23,29,30] in single quantum dots with two "active" levels, where the relevant singlet is a configuration with the lower dot level doubly occupied [31], and consequent Kondo screening arises by a single effective channel [26].}

From the perspective of the two-impurity Anderson model, and its experimental realization in our device, this conductance peak is the signature of the finite-field crossover from a local singlet (LS) phase for $B \lesssim B_c$, to a polarized Kondo screened (KS) phase for $B \gtrsim B_c$, and amounts to a finite-B continuation of the zero-field conductance peak at $J \sim T_K$ [14–17]. For a L-R symmetric two-impurity Kondo model, it was recently shown [14] that

the well known zero-field quantum phase transition between the LS and KS phases, occurring at $J = J_c \sim T_K$, extends into the (B, J)-plane [Fig. 3(c)]. The transition could thus be driven either by tuning J through J_c at zero field, *or* by tuning B through a critical B_c at fixed J. With interlead charge transfer and L-R asymmetry, both of which occur in our device, the transition line is of course broadened into a line of crossovers [Fig. 3(c)] with associated conductance peaks. For $J \gg J_c$ in particular, where the system at zero field is deep in the LS phase, $B_c \sim J/g\mu_B$ (and the Kondo screened phase for $B > B_c$ is naturally spin polarized, asymptotically approaching the free T_- state). This behavior is observed clearly in Fig. 3(d). In the center of the (1,1) regime, $J \sim 0.34$ meV (as estimated above) yields $B_c \sim J/g\mu_B = 2.9$ T, in very good agreement with the measured conductance peak in Fig. 3(d) [18]. As detuning increases, J becomes larger as noted above, and B_c is correspondingly seen to increase. The evolution of conductance as a function of magnetic field is in good agreement with the NRG calculations as shown in Figs. 3(b) and 3(d). The calculations also confirm (not shown) that the asymmetry in V_{sd} observed [Fig. 3(a)] in the differential conductance with increasing detuning results from the asymmetry $\Gamma_L \neq \Gamma_R$. For symmetric coupling strengths, or precisely at the center of the (1,1) charge regime where the system is electron-hole symmetric [e.g., the leftmost plot in Fig. 3(a)], no asymmetry is observed in the differential conductance.

Finally, we show that by varying V_{bar} [see Fig. 1(a)] we can directly tune the coupling strengths between the quantum dots and their leads [32]. This is illustrated in Fig. 4(a) which shows that for decreasing V_{bar}, the conductance at the center of the (1,1) charge regime strongly increases. At the same time, the double peak structure, clearly observed for higher values of V_{bar}, gradually merges into one broad peak. This behavior can be understood as an increase in the coupling strengths $\Gamma_{L,R}$, as illustrated by the NRG calculations, see Fig. 4(b), and consistent with the increase in widths of the Coulomb blockade peaks in the stability diagrams. On increasing $\Gamma_{L,R}$, and hence decreasing $U/\Gamma_{L,R}$, the device becomes less strongly correlated and charge fluctuations consequently more significant, thereby eroding and ultimately destroying the double peak structure that is characteristic of the strongly correlated regime of the DQD.

In conclusion, we have investigated a tunable two-impurity Kondo system in a strongly correlated carbon nanotube DQD, in which the full range of charge regimes is accessible, and which amounts to a clear experimental realization of a two-impurity Anderson model. In the (1,1) regime, we have shown that the exchange and Kondo energy scales can be varied by tuning the dot energy levels or by varying the dot-lead tunnel couplings, providing the possibility of observing the crossover between local singlet and Kondo screened phases. While charge fluctuations in
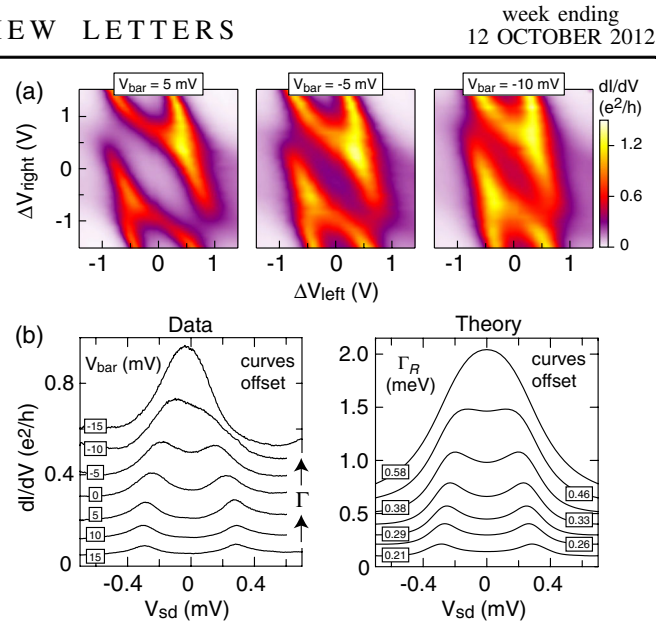

FIG. 4 (color online). (a) Observed stability diagrams of the DQD for different dot-lead coupling strengths as varied by V_{bar}. (b) Left: differential conductance in the center of the (1,1) charge regime for different dot-lead couplings. The curves are offset in steps of 0.05 e^2/h. Right: NRG calculations, with the ratio $\Gamma_R/\Gamma_L = 2$ fixed and Γ_R as indicated (curves again offset in steps of 0.05 e^2/h).

this device prevented observation of the crossover at zero field, we were able to observe it at finite field, indicated by enhanced zero-bias conductance. The work is readily extended to carbon nanotube DQDs coupled to superconducting [33] or ferromagnetic [34] leads. This allows experimental access to rich phase behavior controlled by the interplay between Kondo, exchange, and superconducting correlations, and further highlights the potential of carbon nanotube quantum dots to investigate correlated electron physics.

[1] P. W. Anderson, Phys. Rev. **124**, 41 (1961).
[2] D. Goldhaber-Gordon, H. Shtrikman, D. Mahalu, D. Abusch-Magder, U. Meirav, and M. A. Kastner, Nature (London) **391**, 156 (1998).
[3] S. M. Cronenwett, T. H. Oosterkamp, and L. P. Kouwenhoven, Science **281**, 540 (1998).
[4] J. Nygård, D. H. Cobden, and P. E. Lindelof, Nature (London) **408**, 342 (2000).
[5] A. C. Hewson, *The Kondo Problem to Heavy Fermions* (Cambridge University Press, Cambridge, England, 1993).
[6] S. Alexander and P. W. Anderson, Phys. Rev. **133**, A1594 (1964); P. Gottlieb and H. Suhl, *ibid.* **134**, A1586 (1964).
[7] C. Jayaprakash, H. R. Krishna-murthy, and J. W. Wilkins, Phys. Rev. Lett. **47**, 737 (1981).

[8] B. A. Jones and C. M. Varma, Phys. Rev. Lett. **58,** 843 (1987); Phys. Rev. B **40,** 324 (1989).

[9] I. Affleck and A. W. W. Ludwig, Phys. Rev. Lett. **68,** 1046 (1992).

[10] I. Affleck, A. W. W. Ludwig, and B. A. Jones, Phys. Rev. B **52,** 9528 (1995).

[11] H. Jeong, A. M. Chang, and M. R. Melloch, Science **293,** 2221 (2001).

[12] N. G. Craig, J. M. Taylor, E. A. Lester, C. M. Marcus, M. P. Hanson, and A. C. Gossard, Science **304,** 565 (2004).

[13] J. Bork, Y.-H. Zhang, L. Diekhöner, L. Borda, P. Simon, J. Kroha, P. Wahl, and K. Kern, Nature Phys. **7,** 901 (2011).

[14] F. W. Jayatilaka, M. R. Galpin, and D. E. Logan, Phys. Rev. B **84,** 115111 (2011).

[15] A. Georges and Y. Meir, Phys. Rev. Lett. **82,** 3508 (1999).

[16] W. Izumida and O. Sakai, Phys. Rev. B **62,** 10260 (2000).

[17] E. Sela and I. Affleck, Phys. Rev. Lett. **102,** 047201 (2009).

[18] See Supplemental Material at http://link.aps.org/supplemental/10.1103/PhysRevLett.109.156804 for details of device fabrication, and additional experimental data on the dependence of conductance on applied magnetic field, temperature, and interdot and dot-lead tunnel coupling; together with details of the Hamiltonian used in the NRG calculations, and how the conductance is calculated.

[19] W. J. Liang, M. Bockrath, and H. Park, Phys. Rev. Lett. **88,** 126801 (2002).

[20] M. R. Buitelaar, A. Bachtold, T. Nussbaumer, M. Iqbal, and C. Schönenberger, Phys. Rev. Lett. **88,** 156801 (2002).

[21] F. B. Anders, D. E. Logan, M. R. Galpin, and G. Finkelstein, Phys. Rev. Lett. **100,** 086809 (2008); N. E. Bickers, Rev. Mod. Phys. **59,** 845 (1987).

[22] F. D. M. Haldane, Phys. Rev. Lett. **40,** 416 (1978).

[23] J. Paaske, A. Rosch, P. Wölfle, N. Mason, C. M. Marcus, and J. Nygård, Nature Phys. **2,** 460 (2006).

[24] In the (1,1) regime, $J \simeq \frac{4t^2}{U-U'}[1 - (\epsilon_L - \epsilon_R)^2/(U - U')^2]^{-1}$, and thus increases with detuning ($\epsilon_L - \epsilon_R$).

[25] S. J. Chorley, G. Giavaras, J. Wabnig, G. A. C. Jones, C. G. Smith, G. A. D. Briggs, and M. R. Buitelaar, Phys. Rev. Lett. **106,** 206801 (2011).

[26] M. Pustilnik, Y. Avishai, and K. Kikoin, Phys. Rev. Lett. **84,** 1756 (2000).

[27] M. Pustilnik and L. I. Glazman, Phys. Rev. Lett. **85,** 2993 (2000); Phys. Rev. B **64,** 045328 (2001).

[28] S. Florens, A. Freyn, N. Roch, W. Wernsdorfer, F. Balestro, P. Roura-Bas, and A. A. Aligia, J. Phys. Condens. Matter **23,** 243202 (2011).

[29] D. M. Zumbühl, C. M. Marcus, M. P. Hanson, and A. C. Gossard, Phys. Rev. Lett. **93,** 256801 (2004).

[30] N. Roch, S. Florens, V. Bouchiat, W. Wernsdorfer, and F. Balestro, Nature (London) **453,** 633 (2008).

[31] In our case by contrast, states such as (2, 0) or (0, 2) are $\mathcal{O}(U)$ higher in energy than the (1, 1) states close to the center of the (1, 1) charge regime, and thus irrelevant.

[32] In general, varying the barrier gate voltage affects both the tunnel coupling t and the coupling to the leads. For the charge configuration here the main effect is on the lead couplings.

[33] M. R. Buitelaar, T. Nussbaumer, and C. Schönenberger, Phys. Rev. Lett. **89,** 256801 (2002).

[34] J. R. Hauptmann, J. Paaske, and P. E. Lindelof, Nature Phys. **4,** 373 (2008).